Supplementary Information

Near-infrared emission of a novel nonconventional luminophore for in vitro imaging

Qinbin Zhang [a, 1], Chuan Huang [a, 1], Shilu Huang [a], Haijiao Xie [b], Qing Huang [a*], Mingming Guo [a*]

[a] School of Chemistry and Chemical Engineering, Southwest University, Chongqing 400715, China

[b] Hangzhou Yanqu information Technology Co., Ltd, Hangzhou, Zhejiang Province, 310003, P.R.O.C.

[c] † 1 The two authors contribute to the work equally.

E-mail address: guomm57@swu.edu.cn (M. Guo); bzzqb19990226@163.com

Table of contents

ITA&NMP-0.5M0.5M and ITA&Py-0.5M0.5M) and the individual molecules (ITA-0.5M, NVP-0.5M, NVC-0.5M and Py-0.5M).

Fig. S24 UV-vis spectra of the mixtures (ITA&NVP-0.5M0.5M, ITA&NVC-0.5M0.5M, ITA&NMP-0.5M0.5M and ITA&Py-0.5M0.5M) and the individual molecules (ITA-0.5M, NVP-0.5M, NVC-0.5M and Py-0.5M).

Table S1. The mixtures molar ratios of ITA with DMF and DMSO.

Mixtures	ITA	DMSO	V_{Total} (mL)
ITA&DMF-0.2M0.2M	112.1 mg	77.1 μL	5 mL
ITA&DMF-1M1M	560.4 mg	385.5 μL	5 mL
ITA&DMF-1M2M	560.4 mg	771.0 μL	5 mL
ITA&DMF-1M6M	560.4 mg	2313.1 μL	5 mL
ITA&DMF-1M10M	560.4 mg	3855.2 μL	5 mL
ITA&DMSO-0.2M0.2M	560.4 mg	71.0 μL	5 mL
ITA& DMSO -1M1M	560.4 mg	355.1 μL	5 mL
ITA& DMSO -1M2M	560.4 mg	710.3 μL	5 mL
ITA& DMSO -1M6M	560.4 mg	2130.8 μL	5 mL
ITA& DMSO -1M10M	560.4 mg	3551.4 μL	5 mL

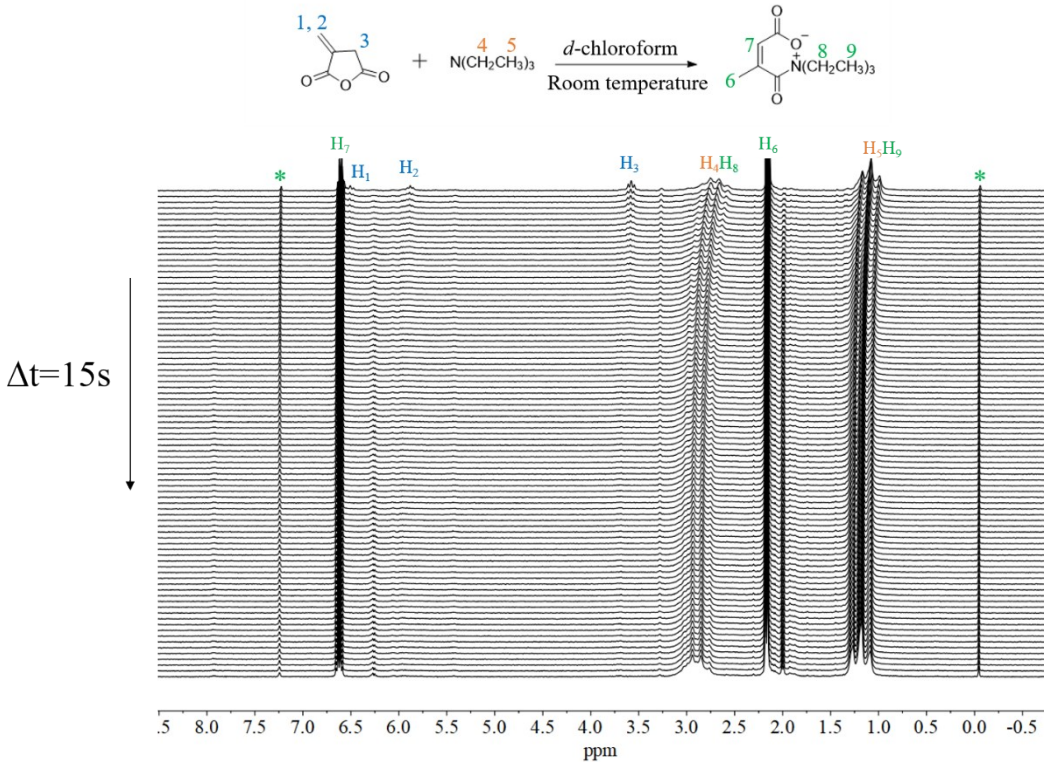

Figure S1. In-situ ^{1}H NMR spectra of the reaction pathway of ITA and TEA (*d*-chloroform).

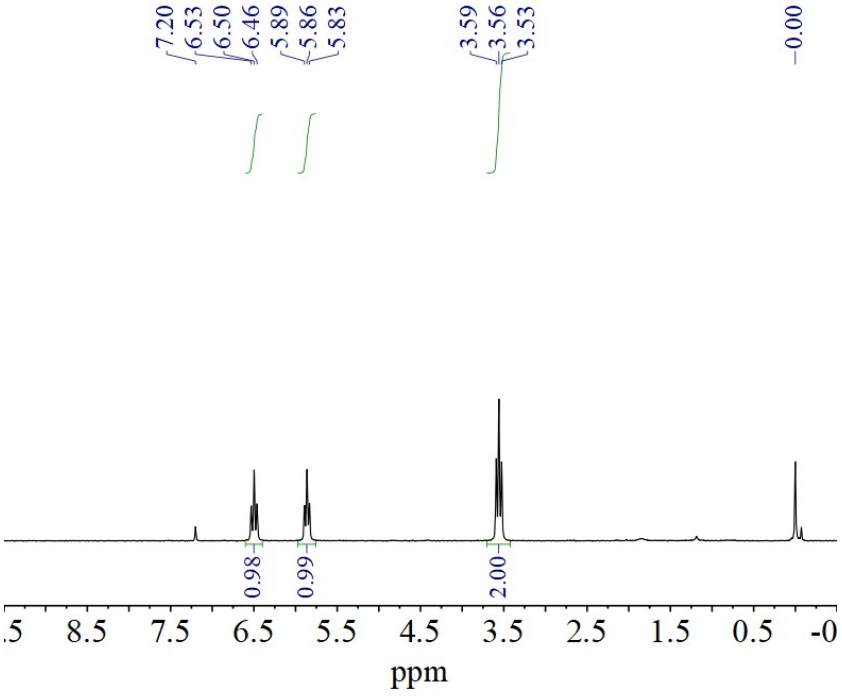

Figure S2. The ^{1}H NMR spectrum of 0.2M ITA in *d*-chloroform.

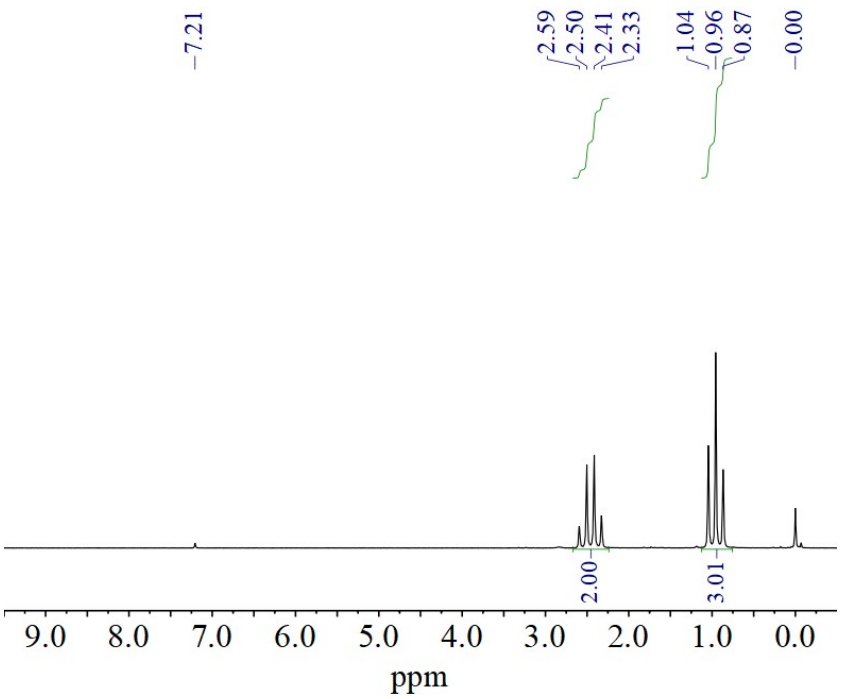

Figure S3. The ^{1}H NMR spectrum of 0.2M TEA in *d*-chloroform.

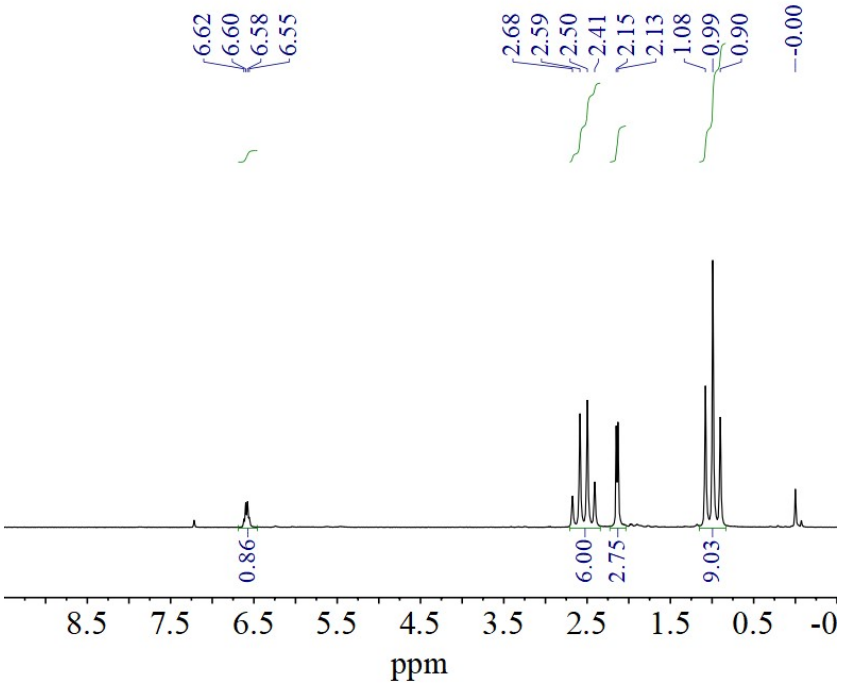

Figure S4. The ^{1}H NMR spectrum of 0.2M I-TEA in *d*-chloroform.

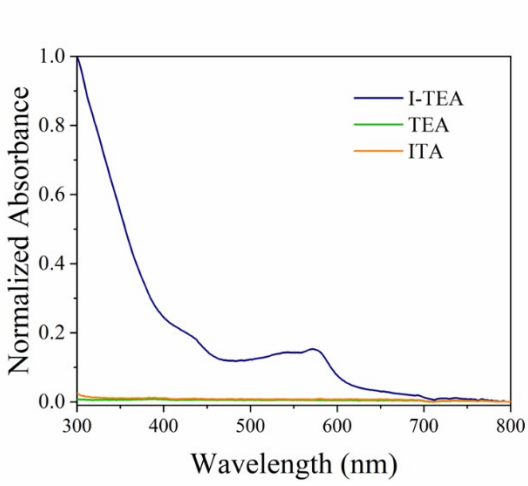

Figure S5. The UV-vis spectra of ITA, TEA and I-TEA

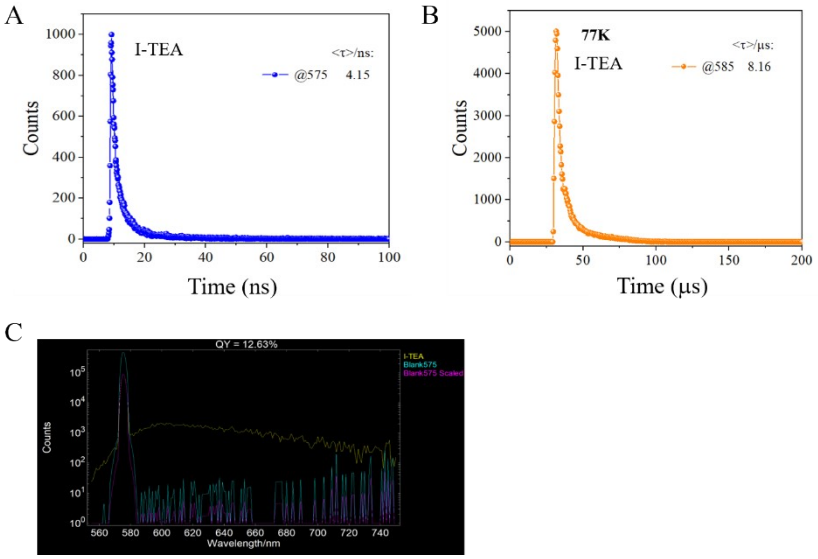

Figure S6. The absolutely quantum yield (C) and ns-scale lifetime decay profile (A) of 1mg/mL I-TEA/DMSO; (B) The μs-scale lifetime decay profile of I-TEA powder at 77K.

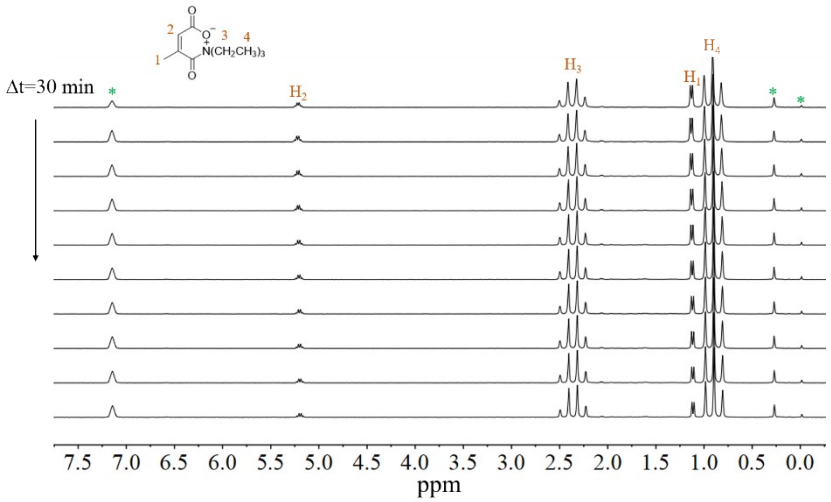

Figure S7. The in-situ ^{1}H NMR spectra of the mixture of ITA and TEA (molar ratio= 1:1). (The "∗" represent the resonance peaks of solvents and TMS)

Table S2. The maximum excitation and emission wavelength of I-TEA at different concentrations

$C_{I\text{-}TEA}$	λ_{max}^{ex} (nm)	λ_{max}^{em} (nm)
1 mg/mL	580	601
10 mg/mL	595	656
20 mg/mL	645	725
40 mg/mL	700	799

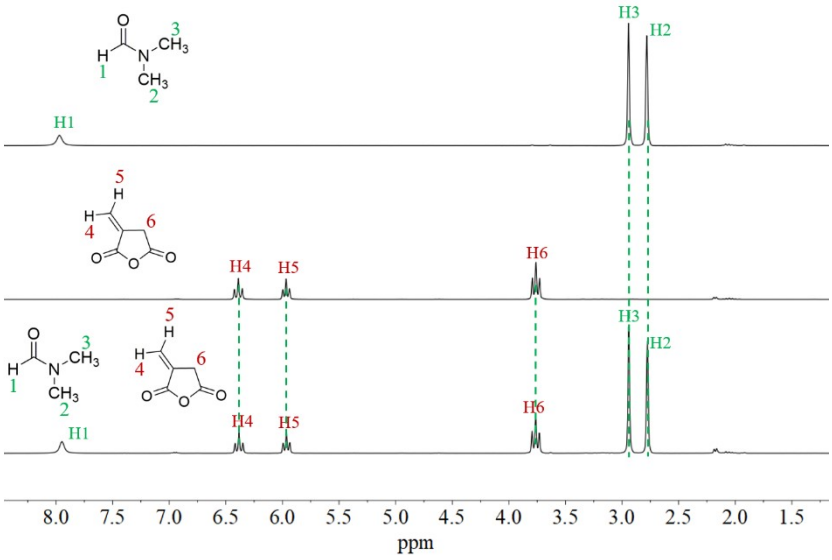

Figure S8. The ^{1}H NMR spectra of ITA-0.2M, DMF-0.2M and ITA&DMF-0.2M0.2M in *d*-acetone.

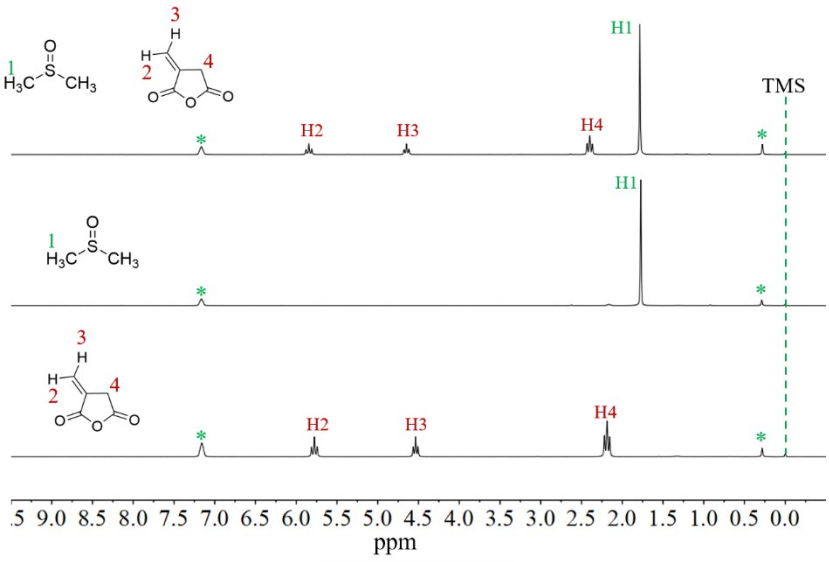

Figure S9. The ^{1}H NMR spectra of ITA-0.2M, DMSO-0.2M and ITA&DMSO-0.2M0.2M in *d*-acetone.

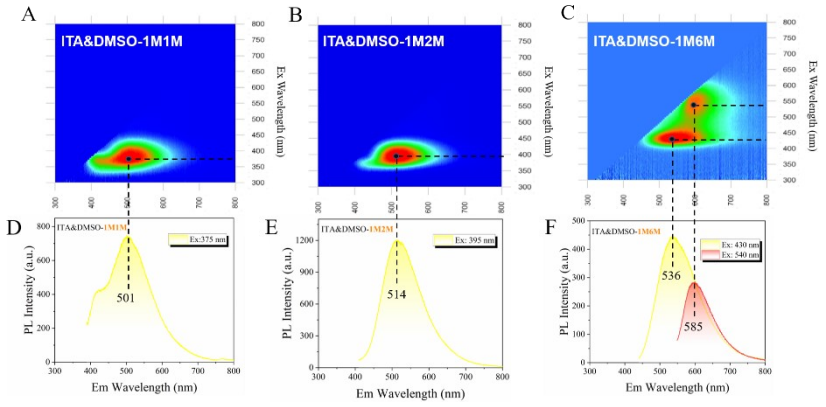

Figure S10. The 3D spectrograms and maximum emission spectra of ITA&DMSO-1M1M, ITA&DMSO-1M2M and ITA&DMSO-1M6M.

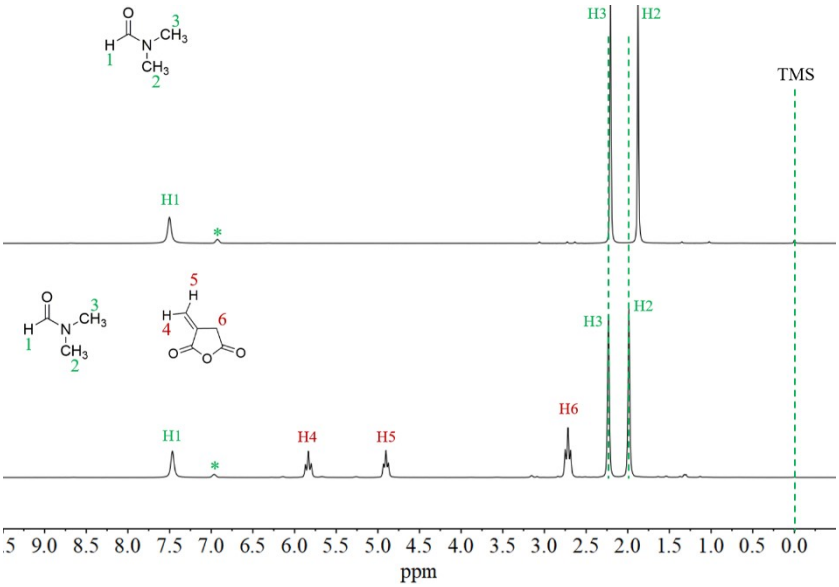

Figure S11. The ^{1}H NMR spectra of DMF-1M and ITA&DMF-1M1M in *d*-benzene.

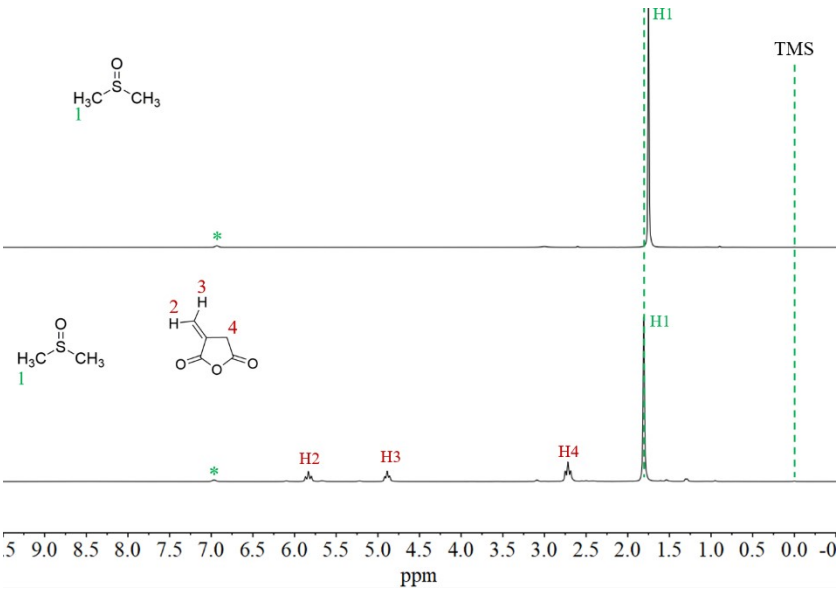

Figure S12. The ^{1}H NMR spectra of DMSO-1M and ITA&DMSO-1M1M in *d*-benzene.

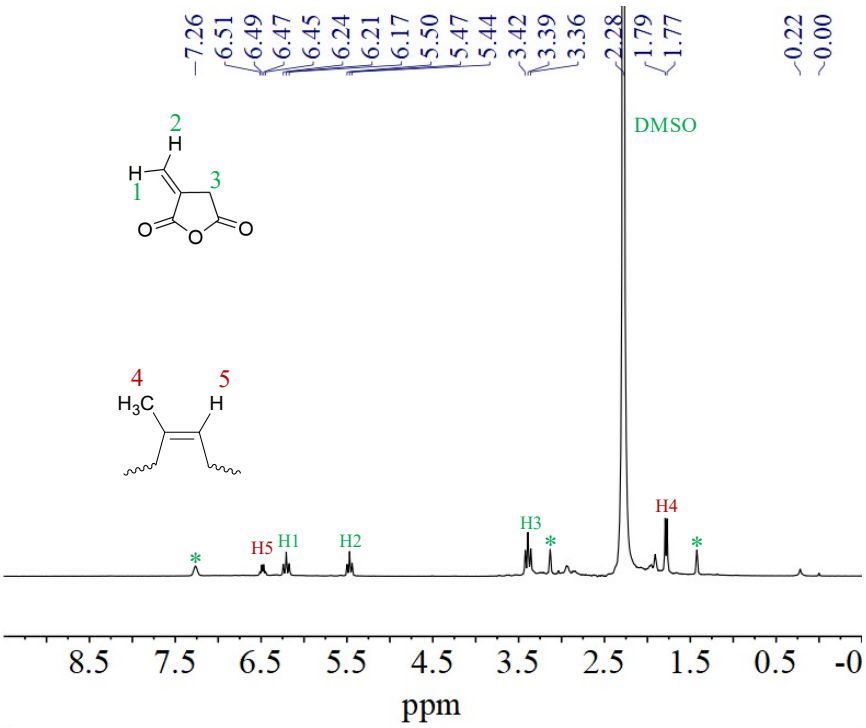

Figure S13. The ^{1}H NMR spectrum of ITA&DMSO-1M6M (*d*-benzene). (The "*" represent the satellite peaks and solvent peak)

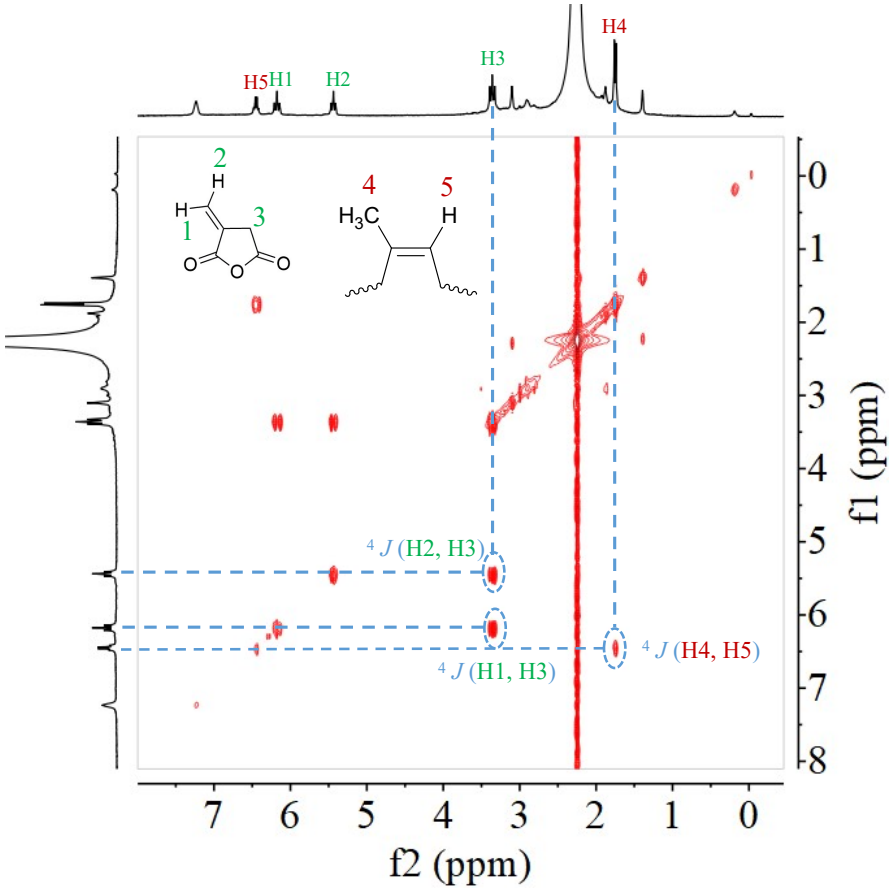

Figure S14. The ^{1}H, ^{1}H-COSY spectrum of ITA&DMSO-1M6M (*d*-benzene).

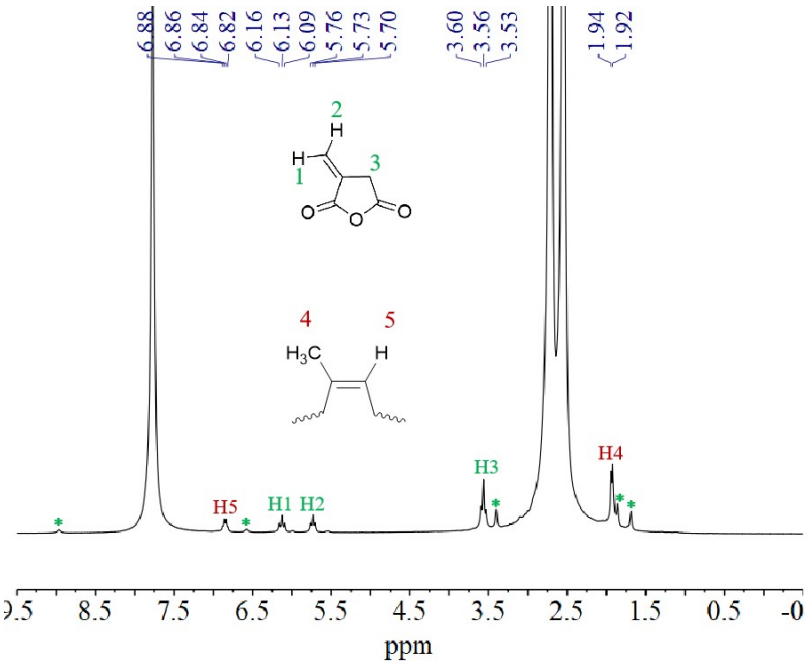

Figure S15. The ^{1}H NMR spectrum of ITA&DMF-1M13M. (The "*" represent the satellite peaks from DMF)

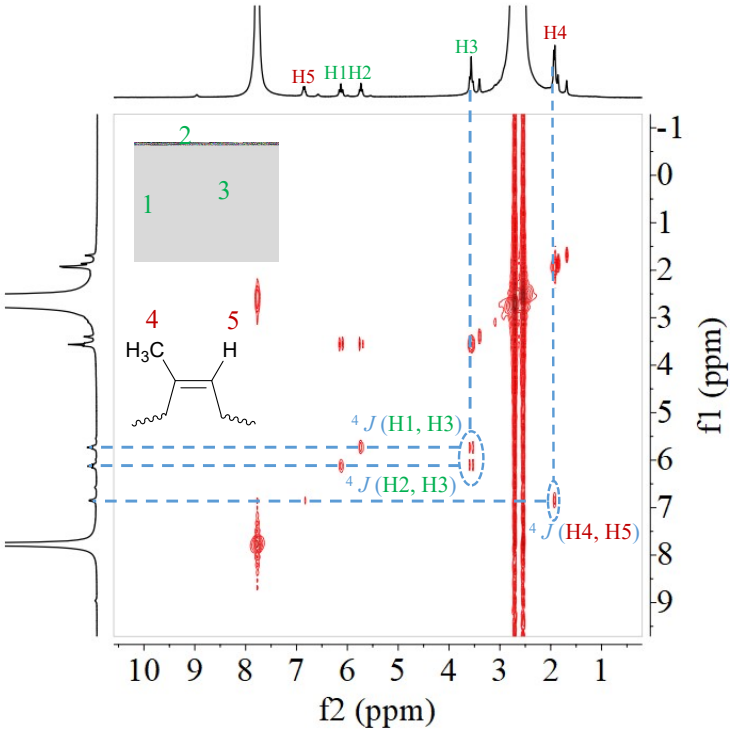

Figure S16. The ^{1}H, ^{1}H-COSY spectrum of ITA&DMF-1M13M.

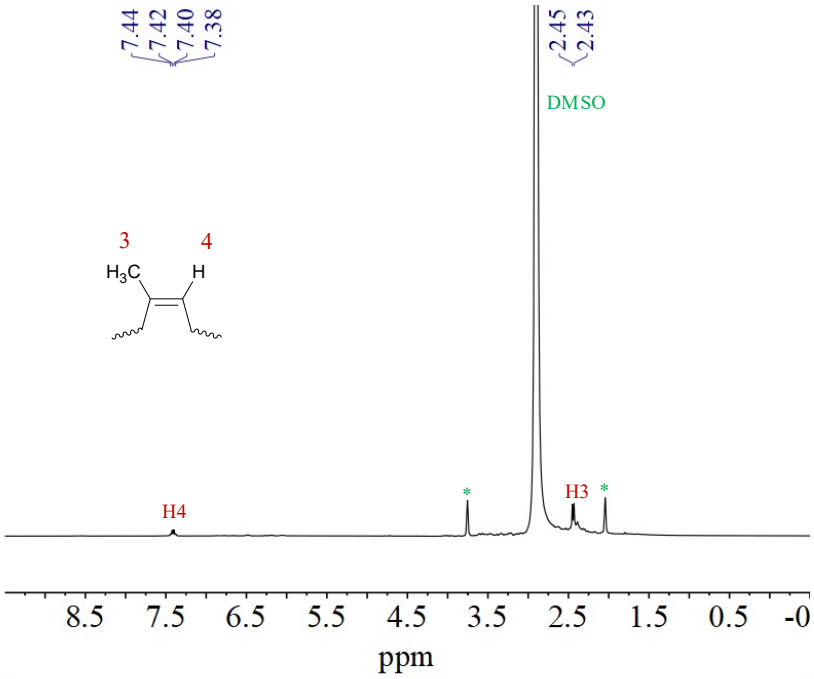

Figure S17. [1]H NMR spectrum of ITA&DMSO-1M14M. (The "∗" represent the satellite peaks)

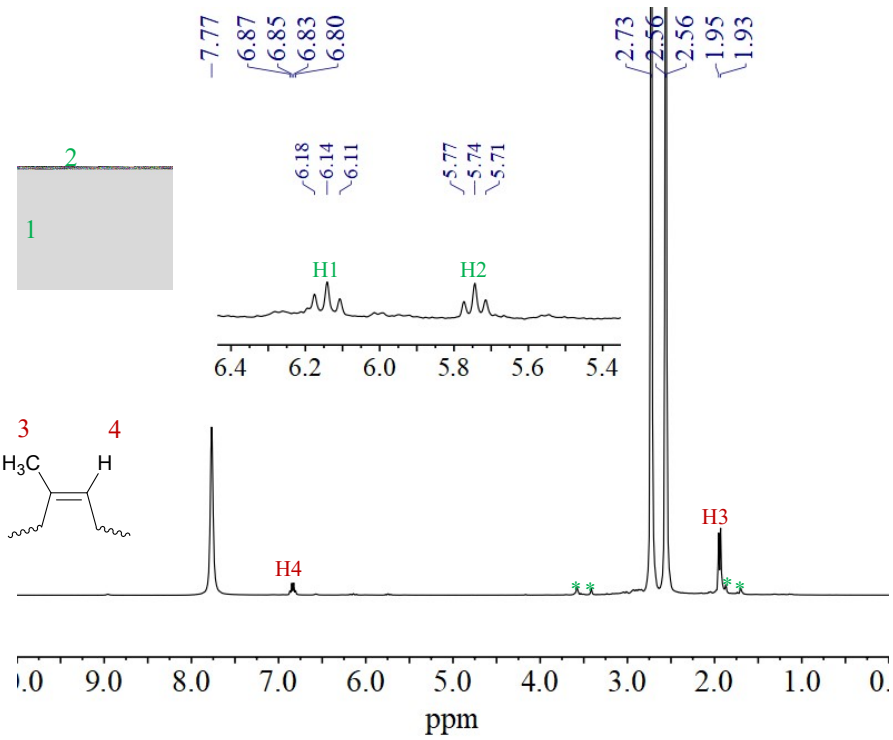

Figure S18. [1]H NMR spectrum of ITA&DMF-2M13M. (The "∗" represent the satellite peaks)

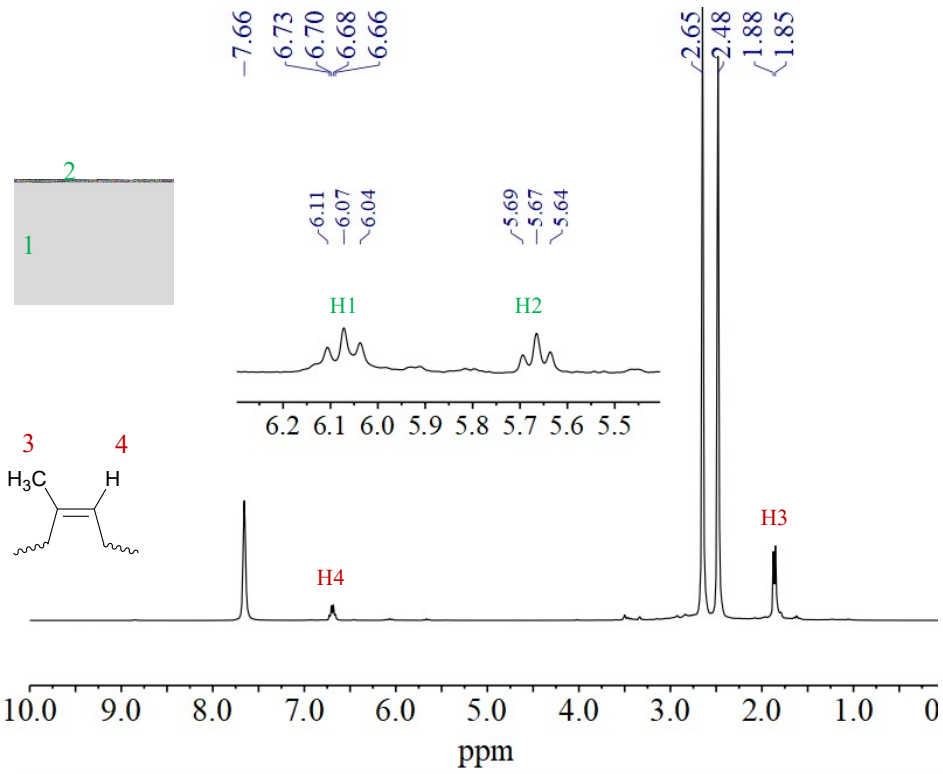

Figure S19. [1]H NMR spectrum of ITA&DMF-4M13M. (The "*" represent the satellite peaks)

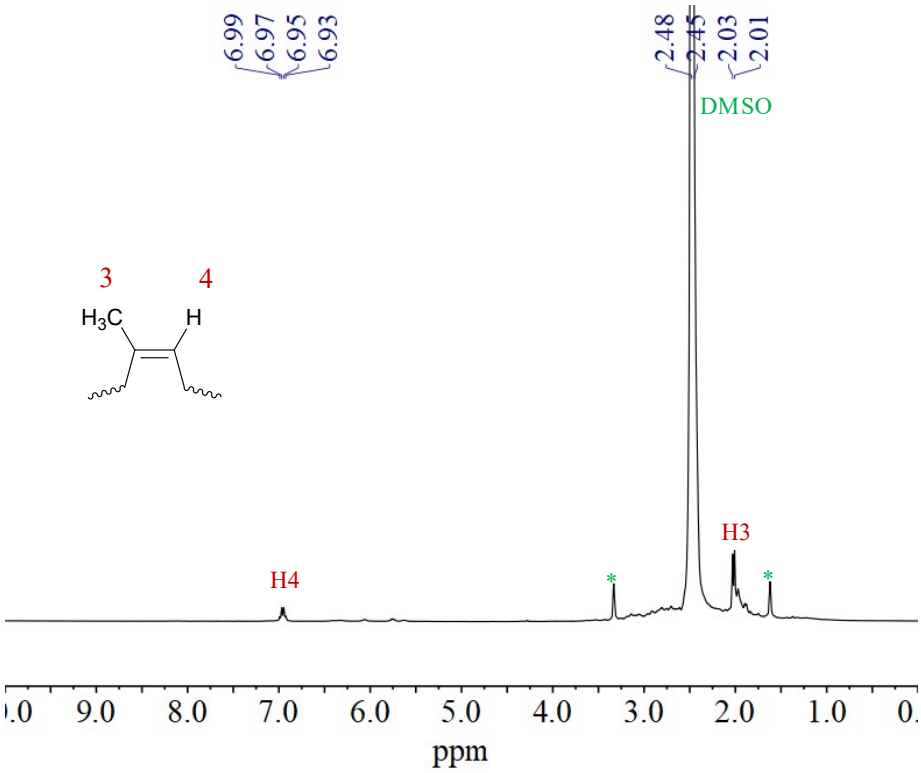

Figure S20. [1]H NMR spectrum of ITA&DMSO-2M14M. (The "*" represent the satellite peaks)

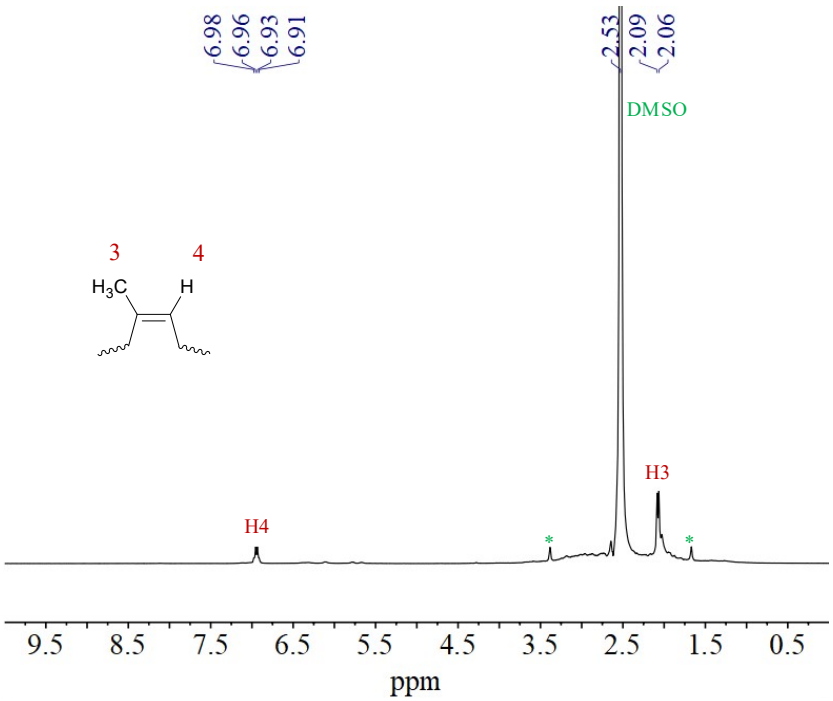

Figure S21. ^{1}H NMR spectrum of ITA&DMSO-4M14M. (The "*" represent the satellite peaks)

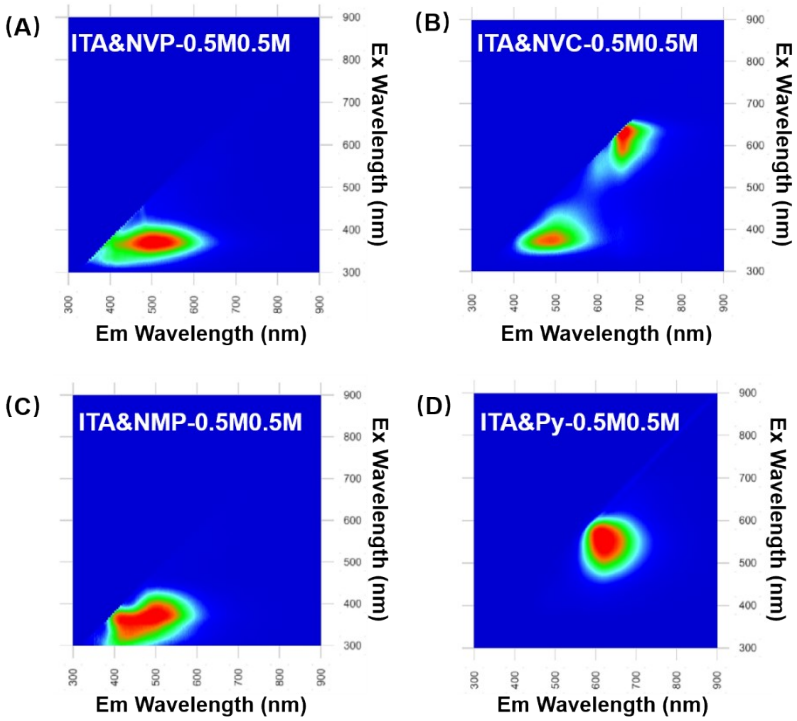

Figure S22. The 3D spectrograms of ITA&NVP-0.5M0.5M, ITA&NVC-0.5M0.5M, ITA&NMP-0.5M0.5M and ITA&Py-0.5M0.5M.

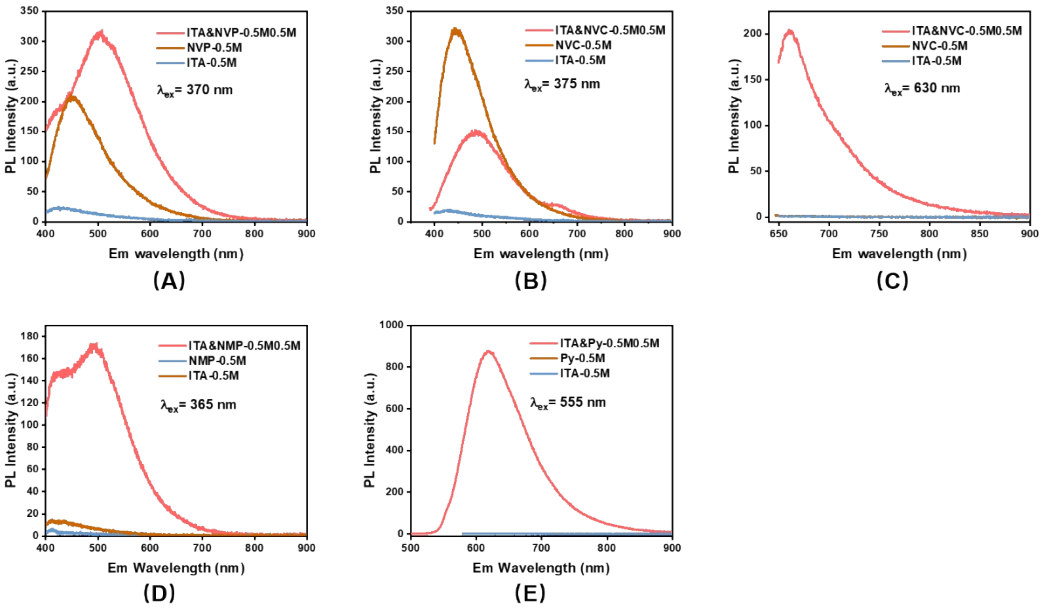

Figure S23. Emission spectra of the mixtures (ITA&NVP-0.5M0.5M, ITA&NVC-0.5M0.5M, ITA&NMP-0.5M0.5M and ITA&Py-0.5M0.5M) and the individual molecules (ITA-0.5M, NVP-0.5M, NVC-0.5M and Py-0.5M).

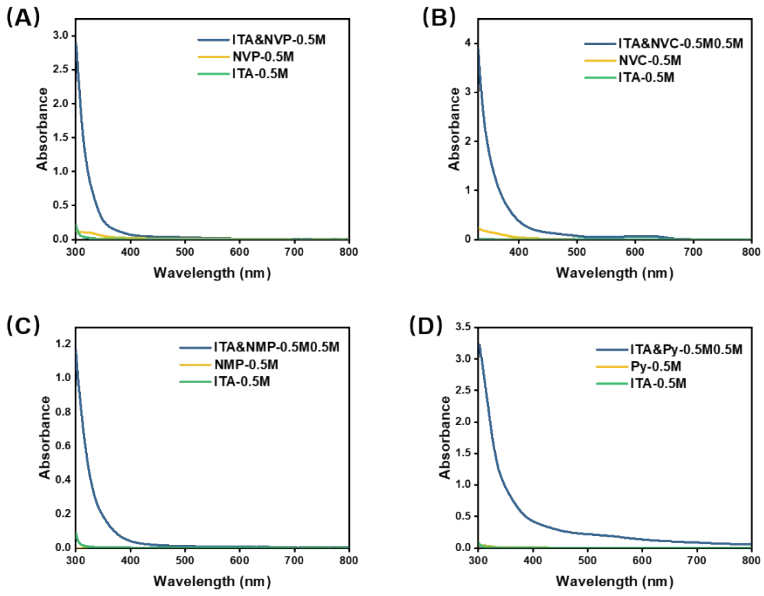

Figure S24. UV-vis spectra of the mixtures (ITA&NVP-0.5M0.5M, ITA&NVC-0.5M0.5M, ITA&NMP-0.5M0.5M and ITA&Py-0.5M0.5M) and the individual molecules (ITA-0.5M, NVP-0.5M, NVC-0.5M and Py-0.5M).

The 3D emission spectra of the mixtures (ITA&NVP-0.5M0.5M, ITA&NMP-0.5M0.5M and ITA&Py-0.5M0.5M) (Supplementary Figure S22 A, C and D) and the emission spectra of the mixtures and individual molecules (ITA&0.5M, NVP-0.5M, NMP-0.5M and Py-0.5M) (Supplementary Figure S23 A, D and E) shown that the mixtures have significant PL characteristics and the emission of the mixtures were not from the individual molecules directly. Meanwhile, the 3D emission spectra of the mixture (ITA&NVC-0.5M0.5M) (Supplementary Figure S22 B) showed

two emission centers, and the emission spectra of mixture and individual molecules (ITA-0.5M and NVC-0.5M) (Supplementary Figure S23 B and C) showed the emission center at the long-wavelength region was not from the individual molecules directly, which demonstrated the presentence of new emission center in the mixture. The UV-vis spectra of all the mixtures and individual molecules (Supplementary Figure S24 A-D) showed the absorbance of the mixtures were stronger than the individual molecules and the absorption of the mixtures were both appeared at the redder region when compared to the individual molecules. These phenomena illustrated the existence of extended conjugation with electron delocalization in the mixtures and thereby giving the PL characteristics to the mixtures.